ACS APPLIED MATERIALS & INTERFACES

Research Article

www.acsami.org

Synthesis of InN@SiO_2 Nanostructures and Fabrication of Blue LED Devices

Anurag Gautam and Frank C. J. M. van Veggel*

Department of Chemistry, University of Victoria, Victoria, British Columbia V8W 3V6, Canada

Supporting Information

ABSTRACT: We synthesized InN@SiO_2 nanostructures (i.e., nanoparticles and nanowires) by varying the annealing temperature and nitridation conditions of In_2O_3@SiO_2 nanoparticles in the presence of ammonia. The In_2O_3@SiO_2 nanoparticles were synthesized using a urea-based homogeneous precipitation of indium hydroxide on the surface of the SiO_2 (15 nm) nanoparticles, followed by annealing at 600 °C in air. Subsequently, nitridation of In_2O_3@SiO_2 nanoparticles in ammonia at 600 °C for 2 h resulted in InN@SiO_2 nanoparticles. The sizes of InN nanoparticles are ∼5 nm on the silica surface. Nitridation at the same temperature for 3−5 h gave InN nanoparticles of size ∼20 nm. Furthermore, on annealing above 650 °C the InN nanoparticles grew in the form of nanowires. The nanowires are 4−5 μm in length and have a diameter of 100 nm. The photoluminescence peak of both InN@SiO_2 nanoparticles and nanowires is centered at 442 nm (λ_{exi} = 325 nm). Subsequently, the surface of InN@SiO_2 nanoparticles was modified by reacting with dodecyltriethoxysilane at 80 °C, which enabled them to be dispersible in toluene. The surface-modified InN@SiO_2 nanoparticles were used to fabricate blue electroluminescence devices which showed blue electroluminescence peak centered at 442 nm. The Commission Internationale de l'Eclairage (CIE) coordinates of InN@SiO_2 nanoparticles are X = 0.15 and Y = 0.13, which is well within the blue region and commercially appropriate.

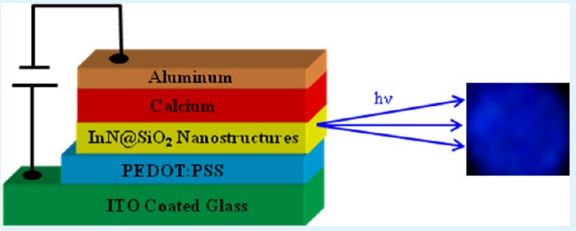

KEYWORDS: *nanoparticles, nanowires, blue electroluminescence, color coordinates*

INTRODUCTION

A significant amount of research has been focused on commercial blue/near UV light sources because of their increased demand in a wide range of applications such as, long-lifetime displays, photolithography, optical data storage, and light-emitting diodes (LEDs).[1−3] LEDs are one of the strongest applications due to many advantages over the conventional incandescent and fluorescent light sources such as, (i) low power consumption, (ii) compact size, (iii) long lifetime and iv) more environmental friendly than the fluorescent light sources.[4,5] Specifically, LEDs fabricated from group III-nitrides such as GaN, and their related alloys like InGaN or InGaAlN have been demonstrated as excellent blue emitters.[6−9] These blue emitting LED technologies have made white LED possible in which the white light is obtained by coating a yellow phosphor ($Y_3Al_5O_{12}$:Ce^{3+} or YaG:Ce)[10] or by coating green/red phosphor ($SrGa_2S_4$:Eu^{2+}/SrS:Eu^{2+})[11,12] on a blue-emitting device. Moreover, the alloy compositions have also been varied to achieve a suitable band gap for producing the desired emission.[13,14] InN had not received much attention initially but currently it has become more attractive material because of its unique properties of high mobility of charge carriers, high saturation velocity, high surface charge accumulation, and low band gap.[15−18] Despite of having the potential applications, InN nanostructures are not well understood because of difficulty in their synthesis, the lower decomposition temperature, and unfavorable Gibb's free energy with respect to indium oxide.[15]

Production of blue light from InN thus remains challenging because of its large surface electron density, which made it extremely difficult to dope, unlike its counterpart GaN, which allows to tune the emission spectrum with respect to doping.[19,20] Several efforts have been employed in preparation of nanosized InN semiconductors;[15−17,21] however, most of the investigations showed the emission from InN nanostructure in the red region.[16,22] There are only a few reports available that have shown emission from InN in the blue region mostly due to existing defect-related emission or due to the hybrid nanostructures.[23−25] Zhang et al.[23] have fabricated uniformly assembled InN nanowires arrays into hexagonally ordered nanochannels of anodic alumina membranes (AAM) through direct reaction between indium and ammonia. These nanowires exhibit a broad blue-green photoluminescence (PL) in the 300−650 nm wavelength range. Deconvolution of the broad peak resulted in two peaks, the major peak was centered at 478 nm. This blue PL was ascribed due to the existence of defects in indium or nitrogen-related vacancies (V_{In} or V_N) or due to the vacancy pairs. Blue cathodoluminescence (CL) was observed by Liu et al.[24] from In−O−N nanospheres, with a peak

Received: April 20, 2012
Accepted: June 27, 2012
Published: June 27, 2012

centered at 454 nm. This blue CL, which is red-shifted compared to the blue PL from In_2O_3, is ascribed to nitrogen incorporation into indium oxide in the form of In−O−N moieties. Recently, Wu et al.[25] have synthesized TiO_2 thin films covered with InN nanoparticles (InN@TiO_2) using a plasma-enhanced chemical vapor deposition (PECVD) technique. The InN@TiO_2 nanostructures exhibit a blue emission peak at 420 nm with a small shoulder into the green at 474 nm. The enhanced emission observed from InN@TiO_2 nanostructures with respect to TiO_2 or InN was ascribed to the existence of a hybrid nanostructure.

Blue emission has been achieved by our group in a potentially low-cost approach.[26−28] Recently,[26] we fabricated blue electroluminescence (EL) devices by coating Eu^{2+}-doped GaN on 15 nm silica beads which showed the blue EL peak centered at 450 nm. The calculated Commission Internationale de l'Eclairage (CIE) coordinates were (X = 0.15, Y = 0.15). Earlier, we had also fabricated blue EL devices by coating InN nanoparticles on 50 nm SiO_2 beads with EL emission peak centered at 460 nm.[28] The InN@SiO_2 nanostructures materials were synthesized via a simple solid state reaction. The strategy applied to grow a shell of In_2O_3 on the surface of silica, followed by nitridation in a flow of NH_3 at 700 ^oC resulted in InN@SiO_2 nanoparticles.[29] The origin of the blue emission is probably due to the nitrogen induced defects near the InN-SiO_2 interface. The calculated CIE coordinates were X = 0.18 and Y = 0.23, which are well within the blue region, but not commercially appropriate.[30]

In this work, we modified the strategy described in our earlier report.[28] The InN nanoparticles were coated on 15 nm silica nanoparticles. The reduced size of silica nanoparticles would decrease the disruption of the active layer thickness (∼100 nm) in the device structures. First, 15 nm SiO_2 beads were prepared by using a ternary microemulsion system.[31] Subsequently, a thin shell of $In(OH)_3$ was grown on silica surface in presence of urea via homogeneous decomposition at 85 ^oC. The precipitation of $In(OH)_3$ nanoparticles started at around pH 2. The as-prepared $In(OH)_3$@SiO_2 nanoparticles were annealed at 600 ^oC for 9 h, which gave In_2O_3@SiO_2 nanoparticles. Furthermore, on nitridation the In_2O_3 nanoparticles were converted to InN nanostructures (i.e., nanoparticles and nanowires) on the SiO_2 nanoparticles surface. The shape and size of InN nanostructures was carefully tuned by varying the annealing temperature and nitridation condition in a flow of ammonia. The annealing temperature and period of nitridation were varied from 600 to 700 ^oC and 2 to 7 h, respectively, to tune the shape of InN nanostructure on SiO_2 nanoparticles surface. The resulting InN@SiO_2 nanostructures were used to fabricate EL devices after treating them with dodecyltriethoxysilane ($C_{12}H_{25}Si(OC_2H_5)_3$, DTES), which enabled them to be dispersible in toluene. The InN@SiO_2 nanostructures were characterized with transmission electron microscopy (TEM), energy-dispersive X-ray spectroscopy (EDS), X-ray diffraction (XRD) analysis, Fourier transform infrared (IR) analysis, electron paramagnetic resonance (EPR) measurement, photoluminescence (PL), and EL analyses of fabricated LEDs.

EXPERIMENTAL SECTION

Chemicals used in the synthesis and characterizations were tetraethyl orthosilicate (TEOS), Igepal CA-520, aqueous ammonium hydroxide (28−30%), indium nitrate (99.98%), europium nitrate (99.99%), urea, potassium bromide, ethanol (99.9%), dodecyltriethoxysilane and Poly(3,4-ethylenedioxythiophene) poly(styrenesulfonate). These were used as received from Sigma-Aldrich. The anhydrous ammonia gas (99.999%) used for the nitridation was purchased from Praxair. Distilled water was used in all the experiments.

Preparation of Bare Silica Nanoparticles. The silica nanoparticles were prepared using a ternary microemulsion system.[31] To 10 mL of cyclohexane, 0.1 M surfactant (Igepal CA-520) was added. Subsequently, 0.09 mL water, 0.1 mL of TEOS, and 0.060 mL of NH_4OH were added. The reaction was allowed to stir for 24 h. The microemulsion was broken to recover the SiO_2 nanoparticles by the addition of the ethanol. The SiO_2 nanoparticles were washed three times with ethanol and finally they were washed a couple of times with distilled water. The average size of the SiO_2 nanoparticles obtained was 15 ± 2 nm.

Preparation of In_2O_3@SiO_2 Nanoparticles. The preparation of In_2O_3@SiO_2 nanoparticles was done following a reported procedure with some modifications.[29] Briefly, 0.6 g of urea was dissolved in water and added to a flask containing 15 mL of 15 nm silica nanoparticles. Then an aqueous solution of $In(NO_3)_3$ was added dropwise to the flask and vigorously stirred at 85 °C for 3 h which resulted in white precipitate. The white precipitate was then purified 3 times in water by centrifugation (at 4500 rpm [2180 g force], Beckman Coulter, Spinchron 15 Centrifuge with F0630 rotator). Finally, the product was dried in the vacuum and annealed at 600 °C for 9 h.

Preparation of InN@SiO_2 Nanoparticles. Approximately, 100 mg of In_2O_3@SiO_2 nanoparticles were put in a quartz crucible. Subsequently the crucible was placed in the middle of an electric furnace (Lindberg). The furnace was heated to 600 °C for half hour in NH_3 flow at a rate of 19 °C min^{-1}. Furthermore, the sample was left at 600 °C for 2 h before it was cooled down to room temperature in NH_3 flow. The ammonia flow was maintained at 20 sccm (cubic centimeter per minute at STP) throughout the process. The details of preparation conditions of nanoparticles and nanowires are given in table 1. Finally,

Table 1. Comparisons of Nitridation Conditions and Shape of the InN@SiO_2 and InN Nanostructures

		nitridation			
sample	sample name	temp (°C)	time (h)	nitridation rate (cm^3/min)	shape
1	InN@SiO_2	600	2	20	nanoparticles
2	InN@SiO_2	600	3	30	nanoparticles
3	InN@SiO_2	600	4	30	nanoparticles
4	InN@SiO_2	600	5	30	nanoparticles
5	InN	600	2	20	nanoparticles
6	InN	600	3	30	nanoparticles
7	InN@SiO_2	700	7	50	nanowires
8	InN	700	7	50	nanowires

the InN@SiO_2 nanoparticles were treated with dodecyltriethoxysilane ($C_{12}H_{25}Si(OC_2H_5)_3$, DTES) at 85 ^oC for 24 h and the mixture was centrifuged (at 4500 rpm [2180 g force] to discard the excess of DTES. After centrifugation the DTES-treated InN@SiO_2 product was dried in vacuum at 65 °C.

Fabrication of Electroluminescence (EL) Device with DTES-Treated InN@SiO_2 Nanoparticles. Devices with a configuration of ITO||PEDOT:PSS||InN@SiO_2(DTES treated) ||Ca||Al were fabricated as follows. First, the indium tin oxide (ITO from Delta Technologies, Stillwater, USA) glass substrate was cleaned by sonication in acetone and then in *iso*-propyl alcohol for 10 min in each solvent and dried at room temperature. Subsequently, poly(3,4-ethylenedioxythiophene) doped with poly(styrene sulfonic acid) (PEDOT:PSS) was spin coated on top of ITO glass substrate and then dried at 110 °C in vacuum. Then, the DTES-treated InN@SiO_2 nanoparticles dispersed in toluene

obtained after sonication of 6 h were spin coated on top of the PEDOT:PSS layers. The nanoparticles were spin-coated on the substrate at 1500 rpm for 30 s. The resulting film was then dried at 65 °C for overnight in a vacuum oven. Finally, the metal cathode (20 nm thick Ca and 150 nm Al) was thermally evaporated onto the nanoparticles layer at 5×10^{-5} Torr using a shadow mask to complete the device. The EL was characterized using an Edinburgh Instruments' FLS 920 fluorescence spectrometer. The light was collected with a fiber optic cable which had one end in the glovebox to collect the light emitted from the sample and other end was inserted in the FLS 920 fluorescence spectrometer.

Photoluminescence (PL) Measurements. Room-temperature PL measurements of all samples were performed using a 325 nm Omnichrome Series 74 He−Cd laser by Melles Griot and 450 W Xe arc lamp. For all the measurements, the detector employed was an R928P Hamamatsu PMT, and the resolution due to the slit apertures was 1 nm. A 370 nm cutoff filter was used to collect the spectra.

X-ray Diffraction Analysis. Approximately 40−50 mg of a sample was placed onto a zero-diffraction quartz plate using ethanol. The X-ray diffraction data were collected over range of 2θ = 20−140 degree. XRD patterns were measured with Cr (30 kV, 15 mA) radiation on a Rigaku Miniflex diffractometer with variable divergence slit, 4.2° scattering slit, and 0.3 mm receiving slit. The scanning step size was 0.5° per minutes.

Transmission Electron Microscopic (TEM) Measurements. A JEOL JEM-1400 tungsten filament up to 80 kV Transmission Electron Microscope was used to collect the TEM images. TEM specimens were prepared by dipping a copper grid (600 mesh) which was coated with an amorphous carbon film into the ethanol dispersion of the nanomaterials composites, followed by drying at room temperature.

Scanning Electron Microscopic (SEM) Measurements and Energy-Dispersive X-ray Spectroscopy (EDS). The EDS analysis was done using a Bruker Quantax EDS system linked to the Hitachi S-4800 field-emission scanning electron microscope. The samples were gently crushed and placed on the sample holder covered with a sticky carbon tape.

Raman Spectroscopy Measurement. Raman spectra were collected by exciting the sample with a 632.8 nm from a He−Ne laser by Melles Griot. The solid sample was evenly spread over a clean glass slide. Each spectrum is an average of six scans with objective of 50 X and collected over 30 s.

Fourier Transform Infrared (FTIR) Measurements. FTIR measurements were done using a Perkin-Elmer FTIR spectrometer 1000 machine. A KBr pellet was made by mixing dried KBr and the sample approximately in the ratio 10:1. All spectra were an average of four scans and recorded with a resolution of 2 cm^{-1}.

RESULTS AND DISCUSSION

The synthesis of silica nanoparticles was done via hydrolysis and condensation of tetraethyl orthosilicate in the presence of surfactant (Igepal CA-520) which produced silica nanoparticles of size 15 nm.[31] Subsequently, a thin layer of indium hydroxide was grown on the silica surface by using a urea-based homogeneous precipitation reaction.[27] This indium hydroxide on surface of SiO_2 nanoparticles was converted to indium oxide nanoparticles by annealing at 600 °C in air for 9 h, which resulted in In_2O_3@SiO_2 nanoparticles. The formation of indium oxide nanoparticles was confirmed by XRD analysis which revealed its presence as the cubic phase (see the Supporting Information, Figure S1).[32] Finally, the lightly yellow colored In_2O_3@SiO_2 nanoparticles were converted to InN@SiO_2 nanostructures in a flow of NH_3 at 600−700 °C. In addition, the InN@SiO_2 nanostructures were treated with dodecyltriethoxysilane (DTES) at 80 °C for 24 h.[33] The DTES-treated InN@SiO_2 nanostructures were dispersible in toluene. Dispersion in toluene would facilitate the industrial processing of LEDs, because many polymers are spin coated from toluene solutions. The crystal structure of InN@SiO_2 nanostructures was determined by XRD analysis. Figure 1a shows the XRD

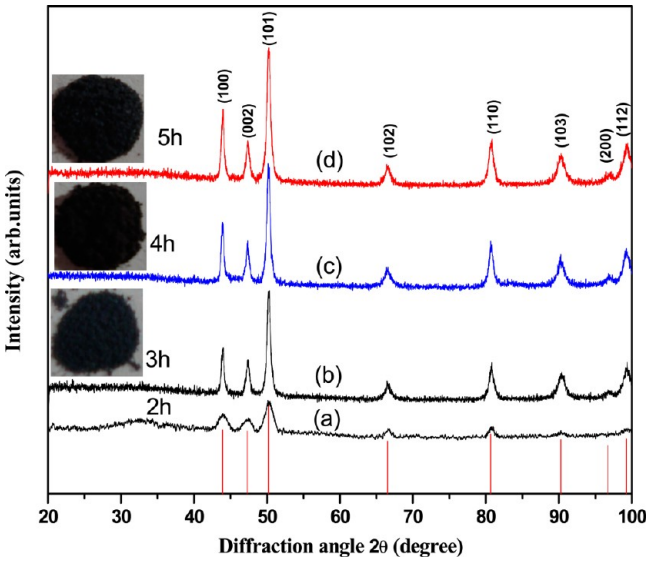

Figure 1. XRD pattern of DTES-treated InN@SiO_2 nanoparticles obtained after nitridation at 600 °C for 2−5 h. The red lines show their standard patterns as in JCPDS card No.792498. The digital images of InN@SiO_2 nanopowders are shown in the inset after 2−5 h of nitridation.

pattern of DTES-treated InN@SiO_2 nanoparticles obtained on nitridation of In_2O_3@SiO_2 nanoparticles at 600 °C for 2 h (Sample 1, Table 1). The broad hump at a 2θ angle of 30° is from the amorphous silica present in the InN@SiO_2 nanoparticles. Furthermore the diffraction peaks appears at angles (2θ) of 43.9, 47.4, 50.3, 66.5, 80.8, 90.3, 96.7, and 99.4 are assigned to be reflections from the (100), (002), (101), (102), (110), (103), (200), and (112) crystal planes respectively (JCPDS Card, file No.792498).[34] This pattern reveals the hexagonal crystal structure (space group $P6_{3mc}$) of InN nanoparticles on silica surface. The crystallite size was found to 5−10 nm as calculated by applying the Scherrer equation. The lattice parameter of InN are a = 0.3531 nm and c = 0.5701 nm agree well with the reported bulk value of InN crystals.[34] The calculated density of InN nanoparticles is 6.94 g/cm^3, which is close to the value of bulk InN (6.92 g/cm^3).[34] The theoretical density is computed by the formula below

$$\text{density} = \{\text{mol wt of InN}\}*Z/[N_A*\{\text{vol of unit cell}\}]$$

Where Z is the number of formula units within the unit cell and N_A is Avogadro's number

On increasing the nitridation period to 3 h (Sample 2, Table 1), the InN nanoparticles grew to 20 nm as calculated from the XRD pattern in Figure 1b. On further extending the nitridation period to 4 and 5 h (sample 3 and 4, Table 1) the size of InN nanoparticles remained the same (Figure 1c, d) as calculated by the Scherrer equation. The color of InN nanopowder is blackish-brown as shown in Figure 1 which remains nearly the same on different hours of nitridation. The growth of InN nanoparticles into nanowires was observed on nitridation temperature above 650 °C. A typical X-ray diffraction patterns of InN@SiO_2 nanowires obtained on nitridation at 700 °C is shown in Figure S2a in the Supporting Information. The separately prepared InN nanowires also show similar XRD

profile as shown in Figure S2b in the Supporting Information. There is no evidence of existence of any In_2O_3 nanoparticles, which confirms complete conversion of the In_2O_3 nanoparticles on the silica surface to InN nanostructures during nitridation. Furthermore the presence of indium metal was not detected by XRD, revealing the formation of well-crystallized InN.

The Raman spectrum of pure SiO_2 nanoparticles obtained after nitridation at 600 ^oC for 3 h is shown in Figure 2a. The

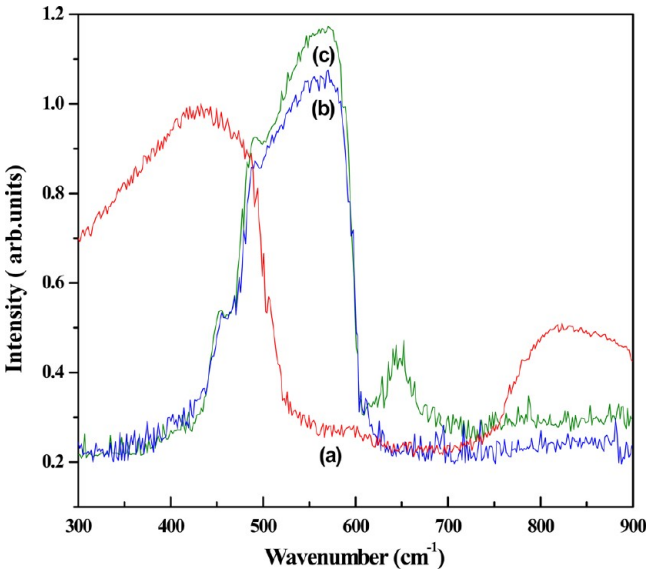

Figure 2. Raman spectrum of (a) SiO_2 nanoparticles, (b) InN@SiO_2 nanoparticles, and (c) DTES-treated InN@SiO_2 nanoparticles obtained after nitridation at 600 °C for 3 h in ammonia.

main Raman peak near 430 cm^{-1} is associated with network bending mode of Si−O−Si vibration. The broad peak at 800 cm^{-1} is assigned to the substantial silicon motion in addition to a bending movement of oxygen.[29,35] The Raman spectrum of InN@SiO_2 nanoparticles (Sample 2, Table 1) is shown in Figure 2b. The peaks at 455 cm^{-1} is assigned as A_1 [Transverse optical (TO)] phonon mode is overlapping with 430 cm^{-1} network bending mode of Si−O−Si vibration. Moreover, the peak at 491 cm^{-1} is assigned to E_2, and the peak at 570 cm^{-1} is assigned to A_1 [longitudinal optical (LO)] phonon mode of the hexagonal crystalline phase of InN.[36,37] The DTES-treated InN@SiO_2 nanoparticles obtained after drying in vacuum at 65 ^oC for 24 h show an additional peak at 650 cm^{-1} in comparison to untreated InN@SiO_2 nanoparticles (Sample 2, Table 1). This peak is assigned to the symmetrical SiO_3 stretching of DTES (Figure 2c).[38] The IR spectrum of the DTES-treated InN@SiO_2 nanoparticles (Sample 2, Table 1) is shown in Figure 3a. The vibrational peak extended over the range of 550−750 cm^{-1} is assigned to InN which is also present in untreated InN@SiO_2 nanoparticles (Figure 3b). DTES-treated InN@SiO_2 nanoparticles have additional vibrational peaks at 2974 and 2856 cm^{-1} which are characteristic of the $-CH_3$ asymmetric and symmetric stretching vibrations in DTES. Furthermore, the vibrational peak at 2928 cm^{-1} is assigned to the asymmetric vibration of the $-CH_2$ groups in DTES[33] and the peaks at 792, 956 1390, and 1466 cm^{-1} are in agreement with the vibrational peaks of DTES, as observed in pure DTES (Figure 3c). The elemental composition of InN@SiO_2 nanoparticles was studied by EDS analysis which confirmed the presence of Si, In, O, and N (see the Supporting

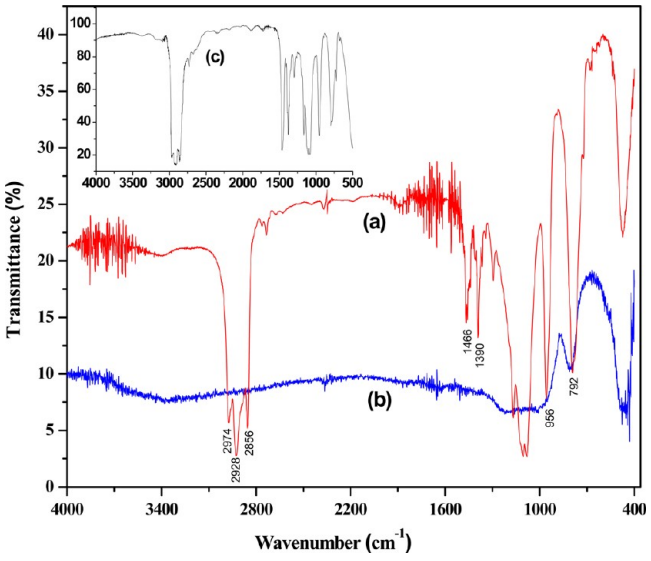

Figure 3. Infrared spectrum of (a) DTES-treated InN@SiO_2 nanoparticles, (b) as-prepared InN@SiO_2 obtained after nitridation at 600 °C for 3 h in ammonia, and (c) pure dodecyltriethoxysilane.

Information, Figure S3). The average of five measurements in a sample gave the atomic proportion of In/N in 1/1.20 ± 0.02. Therefore, the sample is slightly richer in nitrogen than the required for InN. The atomic proportion Si/O is found to be 1/2.50 ± 0.03. The excess of oxygen probably comes from the DTES in which the Si/O atomic proportion is 1:3.[33]

The SEM micrograph of DTES-treated InN@SiO_2 nanoparticles is shown in Figure 4 obtained on nitridation at 600 °C

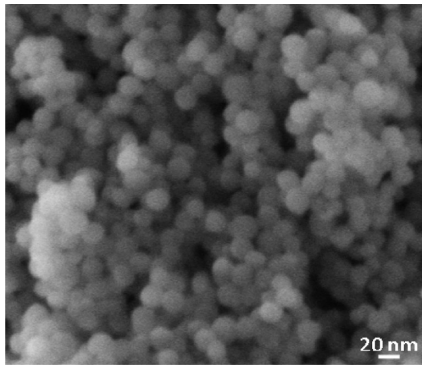

Figure 4. SEM micrograph of DTES-treated InN@SiO_2 nanoparticles obtained on nitridation of In_2O_3@ SiO_2 at 600 °C for 2 h.

for 2 h (Sample 1, Table 1). The InN@SiO_2 nanoparticles are 20 ± 2 nm, as evident from the micrograph. The size of precursor SiO_2 nanoparticles is 15 ± 2 nm as seen in micrographs (see the Supporting Information, Figure S4). Therefore, the estimated sizes of InN nanoparticles coated on SiO_2 surface are of 5−6 nm. These InN nanoparticles are more clearly visible in TEM micrograph of InN@SiO_2 nanoparticles in Figure 5a and DTES-treated InN@SiO_2 nanoparticles in Figure 5b. The small InN nanoparticles coated on the bigger SiO_2 nanoparticles have a size of 5−6 nm, which are comparable to the results obtained by XRD. The micrograph also shows some unattached InN nanoparticles of size 5−6 nm. The InN nanoparticles (Sample 5, Table 1) obtained from nitridation of separately prepared In_2O_3 nanoparticles in the

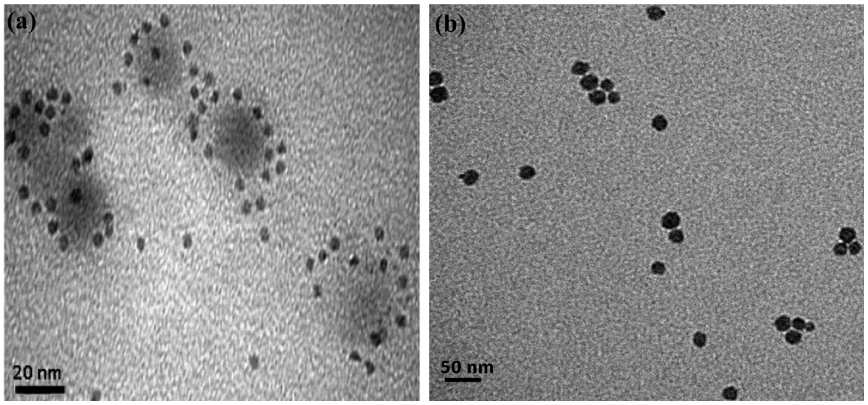

Figure 5. TEM micrograph of (a) InN@SiO_2 and (b) DTES treated of InN@SiO_2 obtained on nitridation at 600 °C for 2 h.

identical condition also show the InN nanoparticles of the same size (see the Supporting Information, Figure S5). On extending the nitridation period to 3 h at 600 °C the size of the InN nanoparticles increase to 20 ± 2 nm (Sample 2, Table 1). The dark black InN nanoparticles in proximity of 15 nm silica beads are clearly visible in the micrograph in Figure 6. The size of InN

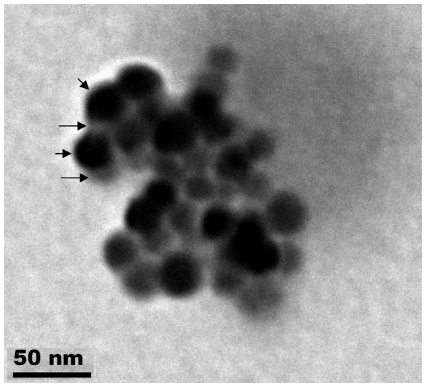

Figure 6. TEM micrograph of DTES-treated InN@SiO_2 nanoparticles obtained on nitridation at 600 °C for 3 h. The smaller and bigger arrows point to InN and SiO_2 nanoparticles, respectively.

nanoparticles agrees well with the result obtained from XRD, which show 20 nm InN nanoparticles. In the similar condition, the size of InN nanoparticles obtained from nitridation of separately prepared In_2O_3 nanoparticles (Sample 6, Table 1) have remained the same (see the Supporting Information, Figure S6). Furthermore on extending the nitridation period of In_2O_3@SiO_2 nanoparticles to 4 and 5 h (Sample 3 and 4, Table 1) there was not much significant variation in the size of InN nanoparticles. A typical TEM micrograph of InN@SiO_2 nanoparticles obtained on nitridation for 4 h is shown in the Supporting Information, Figure S7. The nitridation above 650 °C for 6 h with 50 sccm ammonia flow resulted in InN nanowires. Figure 7a shows the SEM micrograph of DTES-treated InN@SiO_2 nanowires grown at 700 °C (Sample 7, Table 1). The InN nanowires are 4−5 μm long and have diameter between 100 and 110 nm. The very small SiO_2 nanoparticles are not clearly visible in the SEM micrograph, but the EDX analysis confirmed the presence of silicon and oxygen. Therefore, the nanowires are composed of SiO_2 nanoparticles in a matrix of InN, denoated as InN@SiO_2 nanowires. The TEM images of InN@SiO_2 nanowires shown in images b and c in Figure 7 support the result obtained by SEM micrograph. The TEM image in Figure 7b shows InN@SiO_2 nanowires of length 4−5 μm together with smaller ones of 100 nm in length. The higher-magnification TEM image in Figure 7c suggests that the SiO_2 nanoparticles are embedded in InN. The InN nanowires prepared separately (Sample 8, Table 1) under identical conditions also show the InN nanowires of 100−120 nm in diameter and have 4−5 μm in length (see the Supporting Information, Figure S8a, b).

PHOTOLUMINESCENCE AND ELECTROLUMINESCENCE CHARACTERIZATIONS

The photoluminescence of as-prepared and DTES-treated InN@SiO_2 (Sample 1, Table 1) is compared in Figure 8a and b on exciting with the He−Cd laser at 325 nm. The PL emission of the as-prepared InN@SiO_2 nanoparticles (Sample 1, Table 1) shows a blue PL emission peak centered at 442 nm and the emission peak remains unaffected after DTES attachment to the surface of InN@SiO_2 nanoparticles. Furthermore on extending the nitridation period (Sample 2−4, Table 1) we do not see any change in the emission profile. Figure 8c shows the PL emission spectrum of InN nanowires embedded SiO_2 nanoparticles (Sample 7, Table 1). The PL emission peak remains at the same position, as it is for the InN@SiO_2 nanoparticles. The pure InN nanoparticles do not show any emission peak between 350 and 600 nm (Sample 5, Figure 8d) prepared under identical conditions; therefore, the interface with silica plays an important role.[29] The PL spectrum of SiO_2 nanoparticles obtained after nitridation at 700 °C for 7 h shows a weak emission (Figure 7e). This weak emission is possibly due to carbon-related impurities present in SiO_2 nanoparticles, which has been reported earlier.[29,39] The PL emission from the InN@SiO_2 nanoparticles is most likely due to the hybrid interface between InN and SiO_2.[25,29] EDS analysis shows that InN nanoparticles are richer in N than strictly needed for the formation of InN. The richer nitrogen in InN indicates the formation of some type of nitrogen-induced defects or formation of different phases such as oxynitrides at the SiO_2 nanoparticles, particularly at the interface between InN and silica, which is the cause of the blue emission. This is further supported by the InN nanoparticles and InN nanowires, made without any SiO_2, that do not show blue EL.

Figure 9a shows the electroluminescence of DTES-treated InN@SiO_2 nanoparticles and Figure 9b shows the PL emission of as-prepared InN@SiO_2 nanoparticles (Sample1 Table 1). The EL device were fabricated with configuration of ITO|| PEDOT:PSS||InN@SiO_2(DTES-treated)||Ca||Al. Briefly, poly-

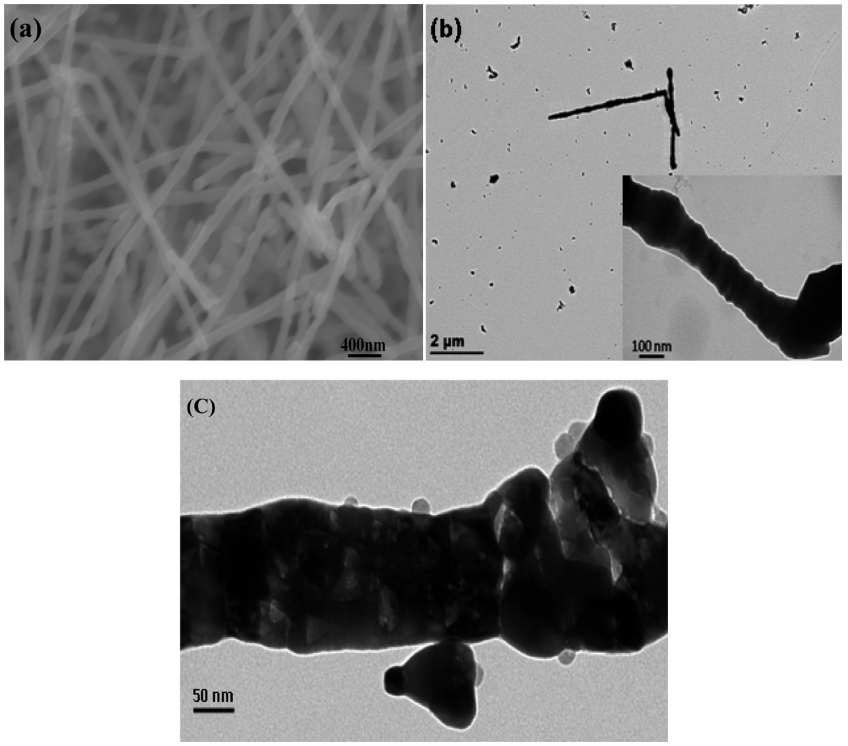

Figure 7. (a) SEM and (b, c) TEM micrograph of DTES-treated InN@SiO_2 nanowires obtained on nitridation at 700 °C for 7 h.

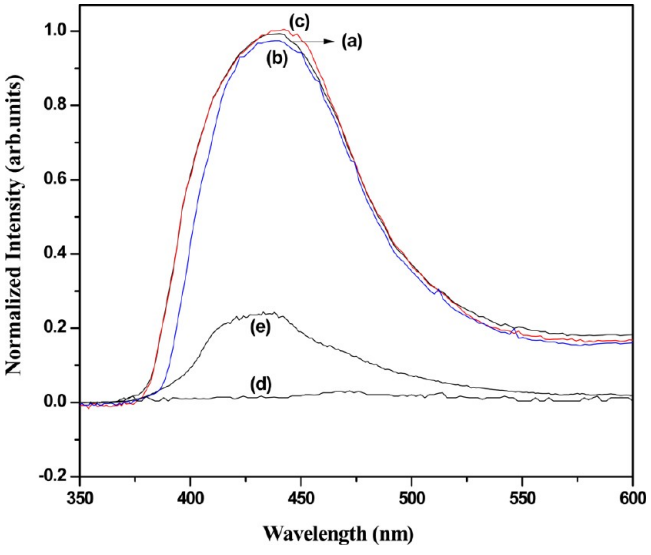

Figure 8. Photoluminescence emission of (a) InN@SiO_2 nanoparticles, (b) DTES-treated InN@SiO_2 nanoparticles after dispersing them in toluene, obtained after nitridation at 600 °C in NH_3 for 2 h, (c) InN@SiO_2 nanowires after nitridation at 700 °C in NH_3 for 7 h, (d) pure InN nanoparticles obtained after nitridation at 600 °C for 2 h, (e) bare SiO_2 nanoparticles after nitridation at 700 °C in NH_3 for 7 h, on exciting it with He−Cd laser operating at 325 nm.

(3,4-ethylenedioxythiophene) doped with poly(styrene sulfonic acid) (PEDOT:PSS) was spin coated on top of cleaned indium tin oxide (ITO) glass substrate and then dried at 110 °C in a vacuum oven. Subsequently, DTES-treated InN@SiO_2 nanoparticles dispersed in toluene were spin coated onto ITO glass substrate. After drying in vacuum, the metallic cathode (Ca protected by Al) was thermally deposited onto the emissive layer with a shadow mask. On applying a 14 V forward bias to the device a blue emission is observed by naked eye and the EL emission spectrum was recorded. The EL emission peak is centered at 442 nm, the same as the PL peak position. The ultimate brightness is of an LED is determined by how fast the excited state decays relative to its formation, so a defect-related mechanism is not necessarily a drawback. This point of view is supported by the nitrogen-induced defect emission devices such as InGaN based LEDs that can be very bright.[40] The emission spectrum does not show any joule heating effect from the fabricated devices having active area ∼7.5 mm^2 and the EL spectrum was reproduced 2 times with the same batch of nanoparticles sample. The calculated EL coordinates were X = 0.15 and Y= 0.13, which fall well within the blue region of 1931 CIE diagram.[30] We also observed the blue emission by the naked eyes from the device fabricated using DTES-treated InN embedded SiO_2 nanowires. The control experiments were also performed under the same conditions having similar configuration using the DTES-treated In_2O_3@SiO_2 and SiO_2 nanocomposites. Their EL emissions are shown in Figure 9c and d, respectively. Control devices did not show any emission on applying 14 V forward bias, clear evidence that supports that the blue emission is most likely originating from the interface of InN and SiO_2 nanostructures in the LED device. This reduced thickness of active emitting layers and dispersibility in toluene would be very helpful in fabricating commercial polymer LEDs.

CONCLUSIONS

In conclusion, we synthesized InN@SiO_2 nanostructures (i.e., nanoparticles and nanowires) by varying the annealing temperature and nitridation condition of In_2O_3@SiO_2 nanoparticles in flow of ammonia. These nanostructures were dispersible in toluene after reacting with DTES. Furthermore, the blue EL device was fabricated using DTES-treated InN@SiO_2 nanoparticles. The EL emission peak was centered at 442 nm, which fall well within the blue region of the CIE color

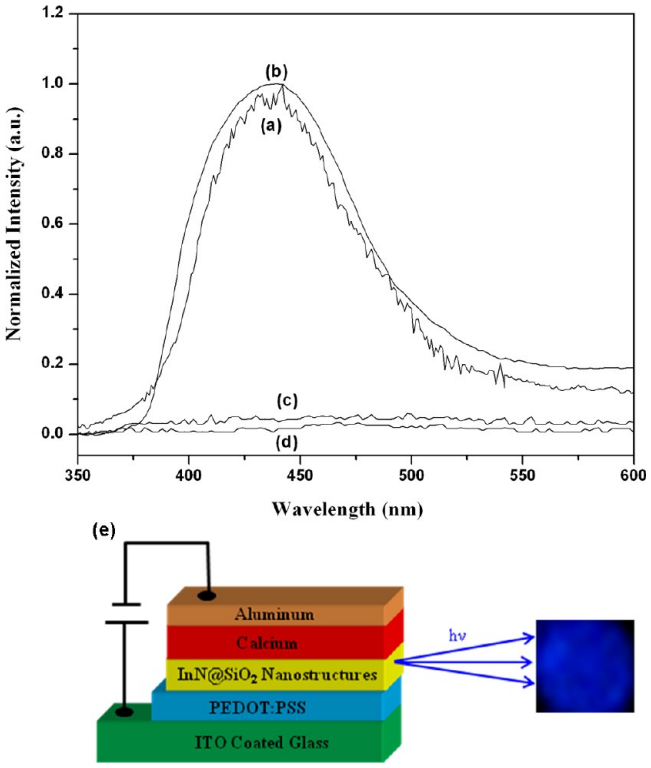

Figure 9. EL emission spectrum collected from (a) ITO||PEDOT:PSS||InN@SiO_2(after reacting with DTES)||Ca||Al device, (b) PL emission spectrum of InN@SiO_2 nanoparticles on nitridation at 600 °C for 2 h, (c) EL emission of spectrum of ITO||PEDOT:PSS||In_2O_3@SiO_2 (after reacting with DTES)||Ca||Al device, (d) EL emission of spectrum of ITO||PEDOT:PSS|| bare SiO_2(after reacting with DTES)||Ca||Al device, SiO_2 nanoparticles used are obtained after nitridation at 700 °C in NH_3 for 7 h, and (e) Fabrication of EL device with the blue emission photograph taken from the device (ITO||PEDOT:PSS||InN@SiO_2(after reacting with DTES)||Ca||Al device).

coordinates graph. The calculated EL emission coordinates of InN@SiO_2 nanoparticles were X = 0.15 and Y = 0.13. This fabrication method of InN@SiO_2 nanoparticles based EL device described here may provide convenient and an economical choice to produce blue light-emitting device.

■ ASSOCIATED CONTENT

Ⓢ Supporting Information

XRD Figure S1 and Figure S2, EDS Figure S3, SEM Figure S4, TEM Figures S5−S7, SEM Figure S8 (PDF). This material is available free of charge via the Internet at http://pubs.acs.org./.

■ AUTHOR INFORMATION

Corresponding Author

*E-mail:fvv@uvic.ca.

Notes

The authors declare no competing financial interest.

■ ACKNOWLEDGMENTS

Funding was provided by the Natural Sciences and Engineering Research Council (NSERC) of Canada, the Canada Foundation for Innovation (CFI), and the British Columbia Knowledge Development Fund (BCKDF) of Canada are gratefully acknowledged for financial support.

■ REFERENCES

(1) Denbaars, S. P. *Proc. IEEE* **1997**, *85*, 1740−1749.
(2) Fasol, G. *Science* **1996**, *272*, 1751−1752.
(3) Steckl, A. J.; Heikenfeld, J. C.; Dong-Seon, L.; Garter, M. J.; Baker, C. C.; Yongqiang, W.; Jones, R. *J. Sel. Top. Quantum Electron.* **2002**, *8*, 749−766.
(4) Kim, J. K.; Schubert, E. F. *Opt. Express* **2008**, *16*, 21835−21842.
(5) Kwon, K. H.; Bin Im, W.; Jang, H. S.; Yoo, H. S.; Jeon, D. Y. *Inorg. Chem.* **2009**, *48*, 11525−11532.
(6) Wu, H.; Zhang, X. M.; Guo, C. F.; Xu, R.; Wu, M. M.; Su, Q. *IEEE Photon. Technol. Lett.* **2005**, *17*, 1160−1162.
(7) Arakawa, Y. *J. Sel. Top. Quantum Electron.* **2002**, *8*, 823−832.
(8) Mahalingam, V.; Sudarsan, V.; Munusamy, P.; van Veggel, F. C. J. M.; Wang, R.; Steckl, A. J.; Raudsepp, M. *Small* **2008**, *4*, 105−110.
(9) Mahalingam, V.; Bovero, E.; Munusamy, P.; van Veggel, F. C. J. M.; Wang, R.; Steckl, A. J. *J. Mater. Chem.* **2009**, *19*, 3889−3894.
(10) Nakamura, S.; Mukai, T.; Senoh, M. *Appl. Phys. Lett.* **1994**, *64*, 1687−1689.
(11) Huh, Y. D.; Shim, J. H.; Kim, Y.; Do, Y. R. *J. Electrochem. Soc.* **2003**, *150*, H57−H60.
(12) Uheda, K.; Hirosaki, N.; Yamamoto, Y.; Naito, A.; Nakajima, T.; Yamamoto, H. *Electrochem. Solid State Lett.* **2006**, *9*, H22−H25.
(13) Matsuoka, T. *Adv. Mater.* **1996**, *8*, 469−479.
(14) Hahn, C.; Zhang, Z.; Fu, A.; Wu, C. H.; Hwang, Y. J.; Gargas, D. J.; Yang, P. *Acs Nano* **2011**, *5*, 3970−3976.
(15) Lan, Z. H.; Wang, W. M.; Sun, C. L.; Shi, S. C.; Hsu, C. W.; Chen, T. T.; Chen, K. H.; Chen, C. C.; Chen, Y. F.; Chen, L. C. *J. Cryst. Growth* **2004**, *269*, 87−94.
(16) Sardar, K.; Deepak, F. L.; Govindaraj, A.; Seikh, M. M.; Rao, C. N. R. *Small* **2005**, *1*, 91−94.
(17) Ashok, V. D.; Ghoshal, T.; De, S. K. *J. Phys. Chem. C* **2009**, *113*, 10967−10974.
(18) Lan, Z. H.; Liang, C. H.; Hsu, C. W.; Wu, C. T.; Lin, H. M.; Dhara, S.; Chen, K. H.; Chen, L. C.; Chen, C. C. *Adv. Funct. Mater.* **2004**, *14*, 233−237.
(19) Chang, Y.-L.; Mi, Z.; Li, F. *Adv. Funct. Mater.* **2010**, *20*, 4146−4151.
(20) Lin, C.-N.; Huang, M. H. *J. Phys. Chem. C* **2009**, *113*, 925−929.
(21) Gao, L.; Zhang, Q.; Li, J. *J. Mater. Chem.* **2003**, *13*, 154−158.
(22) Schofield, P. S.; Zhou, W.; Wood, P.; Samuel, I. D. W.; Cole-Hamilton, D. J. *J. Mater. Chem.* **2004**, *14*, 3124−3126.
(23) Zhang, J.; Xu, B.; Jiang, F.; Yang, Y.; Li, J. *Phys. Lett. A* **2005**, *337*, 121−126.
(24) Liu, B.; Chen, X.; Yao, J. *Nanotechnology* **2007**, *18*, 195604.
(25) Wu, C.-W.; Lu, C.-W.; Lee, Y.-P.; Wu, Y.-J.; Cheng, B.-M.; Lin, M. C. *J. Mater. Chem.* **2011**, *21*, 8540−8542.
(26) Gautam, A.; van Veggel, F. C. J. M. *Chem. Mater.* **2011**, *23*, 4817−4823.
(27) Mahalingam, V.; Tan, M.; Munusamy, P.; Gilroy, J. B.; Raudsepp, M.; van Veggel, F. C. J. M. *Adv. Funct. Mater.* **2007**, *17*, 3462−3469.
(28) Tan, M.; Munusamy, P.; Mahalingam, V.; van Veggel, F. C. J. M. *J. Am. Chem. Soc.* **2007**, *129*, 14122−14123.
(29) Munusamy, P.; Mahalingam, V.; van Veggel, F. C. J. M. *Eur. J. Inorg. Chem.* **2008**, 3728−3732.
(30) *Light Emitting Diodes (Leds) for General Illumination: An Oida Technology Roadmap Updates 2002*; Http://Lighting.Sandia.Gov/Lightingdocs/Oida_Ssl_Led_Roadmap.
(31) Bagwe, R. P.; Yang, C.; Hilliard, L. R.; Tan, W. *Langmuir* **2004**, *20*, 8336−8342.
(32) Chang, S.-C.; Huang, M. H. *J. Phys. Chem. C* **2008**, *112*, 2304−2307.
(33) Dubois, L. H.; Zegarski, B. R. *J. Am. Chem. Soc.* **1993**, *115*, 1190−1191.
(34) *X-Ray Powder Diffraction File*; Joint Committee on Powder Diffraction Standard-International Centre for Diffraction Data: Swarthmore, PA, 1999.
(35) Berrier, E.; Zoller, C.; Beclin, F.; Turrell, S.; Bouazaoui, M.; Capoen, B. *J. Phys. Chem. B* **2005**, *109*, 22799−22807.

(36) Kryliouk, O.; Park, H. J.; Won, Y. S.; Anderson, T.; Davydov, A.; Levin, I.; Kim, J. H.; Freitas, J. A., Jr. *Nanotechnology* **2007**, *18*, 135606.
(37) Chang, S.-C.; Huang, M. H. *Inorg. Chem.* **2008**, *47*, 3135−3139.
(38) Posset, U.; Lankers, M.; Kiefer, W.; Steins, H.; Schottner, G. *Appl. Spectrosc.* **1993**, *47*, 1600−1603.
(39) Canham, L. T.; Loni, A.; Calcott, P. D. J.; Simons, A. J.; Reeves, C.; Houlton, M. R.; Newey, J. P.; Nash, K. J.; Cox, T. I. *Thin Solid Films* **1996**, *276*, 112−115.
(40) Meneghini, M.; Vaccari, S.; Trivellin, N.; Zhu, D. D.; Humphreys, C.; Butendheich, R.; Leirer, C.; Hahn, B.; Meneghesso, G.; Zanoni, E. *IEEE Trans. Electron Device* **2012**, *59*, 1416−1422.